Indian Journal of Pure & Applied Physics
Vol. 52, December 2014, pp. 839-845

Structure, surface morphology and optical properties of $BaTiO_3$ powders prepared by wet chemical method

R Sengodan[1] B Chandar Shekar[2*] & S Sathish[2]

[1]Department of Physics, Kumaraguru College of Technology, Coimbatore, Tamil Nadu

[2] Nanoscience Research Laboratory, Departments of Physics, Kongunadu Arts and Science College, G N-Mills, Coimbatore, Tamil Nadu

*E-mail**:** chandar.bellan@gmail.com

Received 25 September 2013; revised 10 March 2014; accepted 28 October 2014

Barium titanate powders were synthesized by the wet chemical method using the starting materials barium chloride ($BaCl_2$), titanium dioxide (TiO_2) and oxalic acid with different calcinations temperature. The XRD pattern of $BaTiO_3$ calcined at 500 ˚C showed cubic phase whereas $BaTiO_3$ samples calcined at 700 ˚C and above showed tetragonal phase.. The crystallite size, strain and dislocation density were calculated from the XRD spectrum. It was found that crystallite size increases with increase of calcination temperature. EDS spectrum was used to identify the composition of the material. Absorption co-efficient (α), extinction co-efficient (K) and optical band gap were estimated from the optical reflectance spectrum. The band gap of the powder was found to be decreasing with the increase of calcination temperature. Nanoparticles of both spherical and rod like in shape were clearly observed in the SEM.

Keywords: Ferroelectric materials, Wet chemical method, X-ray diffraction, Optical properties

1 Introduction

Ferroelectrics are materials which have the outstanding property of possessing spontaneous electric polarization and the reversibility of the permanent polarization by an electric field. As they possess large piezoelectric values, these are used in different piezoelectric applications[1]. $BaTiO_3$ is an ferroelectric and piezoelectric material with an extensive application. It can be used as a capacitor, thermistor, transducer, transducer, accelerometer or degausser of colour television[2]. Barium titanate (also termed as barium titanium oxide – BTO) appears as a white crystal with a tetragonal crystal structure with a photorefractive effect and piezoelectric properties[3]. Due to the desirable properties and applications, over the last few decades, synthesis of $BaTiO_3$ powders has attracted great attention. Most of the experimental work carried out so far relate to preparation of powders using polymeric precursor method[4] co-precipitation, alkoxide hydrolysis[5], metal-organic processing[6], hydrothermal treatment[7] and the solid state reaction of mixed oxide route[8] etc. Wet chemical method is a promising technique that offers relative low cost, uniform size and homogenous powders. Hence, $BaTiO_3$ powders have been prepared at different calcination temperatures by simple and cost effective wet chemical method in the present study.

2 Experimental Details

$BaTiO_3$ powders were synthesized by using wet chemical method. The starting materials used were barium chloride ($BaCl_2.2H_2O$), titanium dioxide (TiO_2) powder and oxalic acid. The solution of

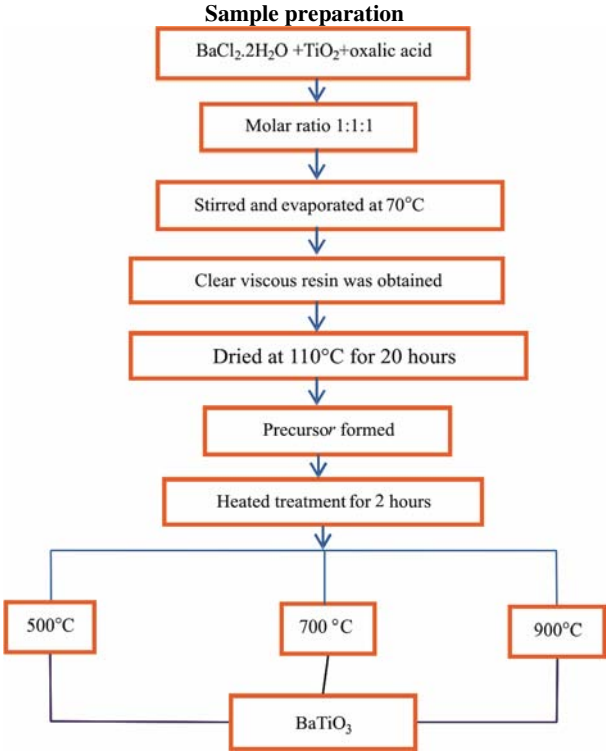

barium chloride, titanium dioxide and oxalic acid in the molar ratio of 1: 1: 1 was stirred and evaporated at 70 ˚C till a clear and viscous resin was obtained. The resin was then dried at 110 ˚C for 20 h. The precursor formed was heated at 500 ˚C, 700 ˚C and 900 ˚C for 2h each. Then, it was brought to the room temperature to form $BaTiO_3$ powders.

2.1 Characteristics of $BaTiO_3$ nanoparticles

The XRD patterns of the resulting particles were obtained from X-ray powder diffractometer with CuKα radiation. The micrograph of $BaTiO_3$ was examined by direct observation via scanning electron microscope (SEM). For optical analysis, JASCO-UV/VISIBLE spectrophotometer (Model Jasco Corp, V-570) was used to get information in the UV and Visible regions.

3 Results and Discussion

3.1 EDS analysis

Figures 1-3 show the EDS spectrum of the $BaTiO_3$ powders at different calcination temperatures. Elemental composition analysis indicated the presence of Ba, Ti and O in the synthesized $BaTiO_3$ powders. High intensity peaks corresponding to Ba, Ti and O elements were clearly noticed in the EDS patterns of the samples calcined at 500 ˚C, 700 ˚C and 900 ˚C. The relative intensities of the peaks corresponding to the Ba and Ti have been found to increase corresponding with increase of calcination temperatures.

3.2 SEM Analysis

SEM images of $BaTiO_3$ particles synthesized at different calcination temperatures are shown in Figs 4-6. The particle synthesized at 500 ˚C and 700 ˚C calcination temperature appears to be of very uniform spherical morphology. In the case of 900 ˚C calcination temperature, some of the particles were transformed to a rod like morphology.

3.3 X-ray diffraction analysis

Figure 7 shows the XRD pattern of $BaTiO_3$ powders calcined at different temperature for 2 h. The XRD pattern of $BaTiO_3$ powder calcinated at 500 ˚C showed cubic structure. Samples calcinated at 700 ˚C and 900 ˚C showed tetragonal structure, which is

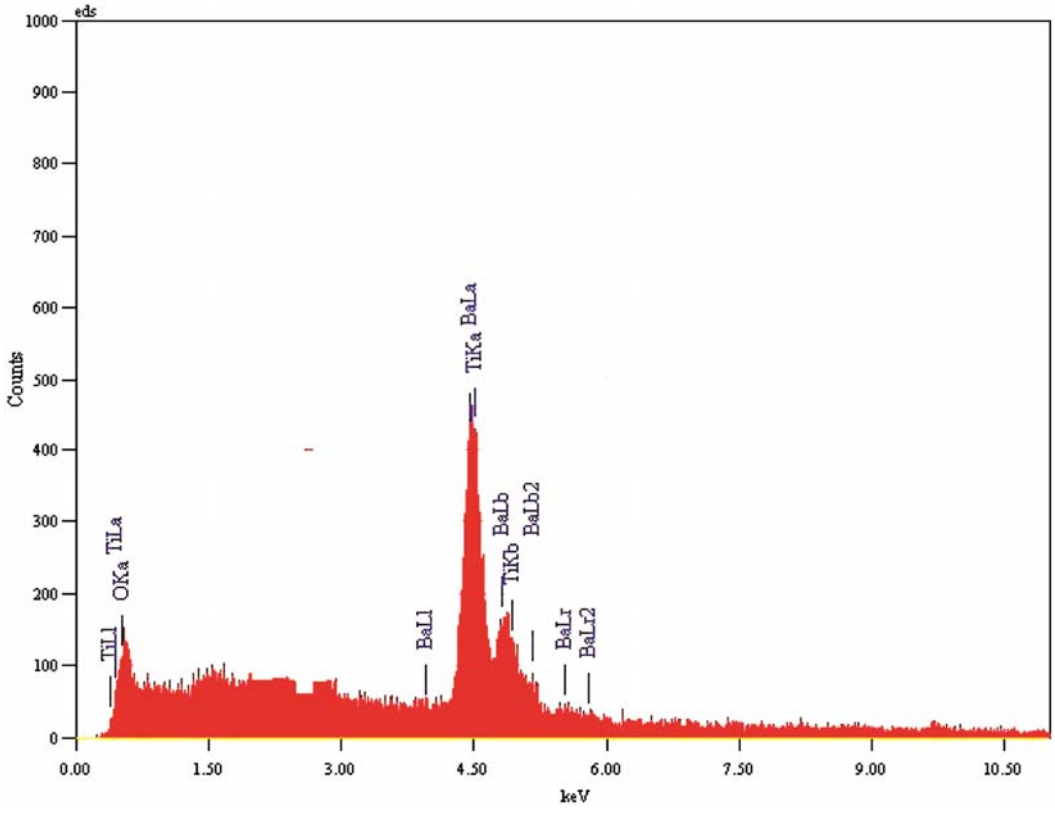

Fig. 1 — EDS spectrum of $BaTiO_3$ powered calcined at 500 ˚C

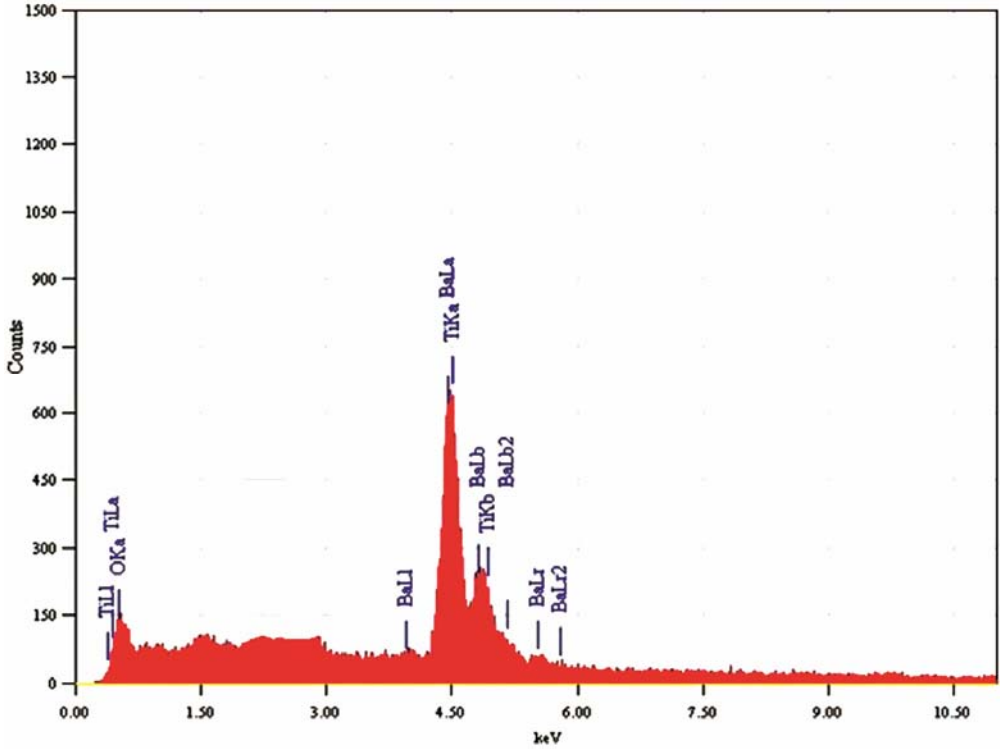

Fig. 2 — EDX spectrum of $BaTiO_3$ powder calcined at 700 °C

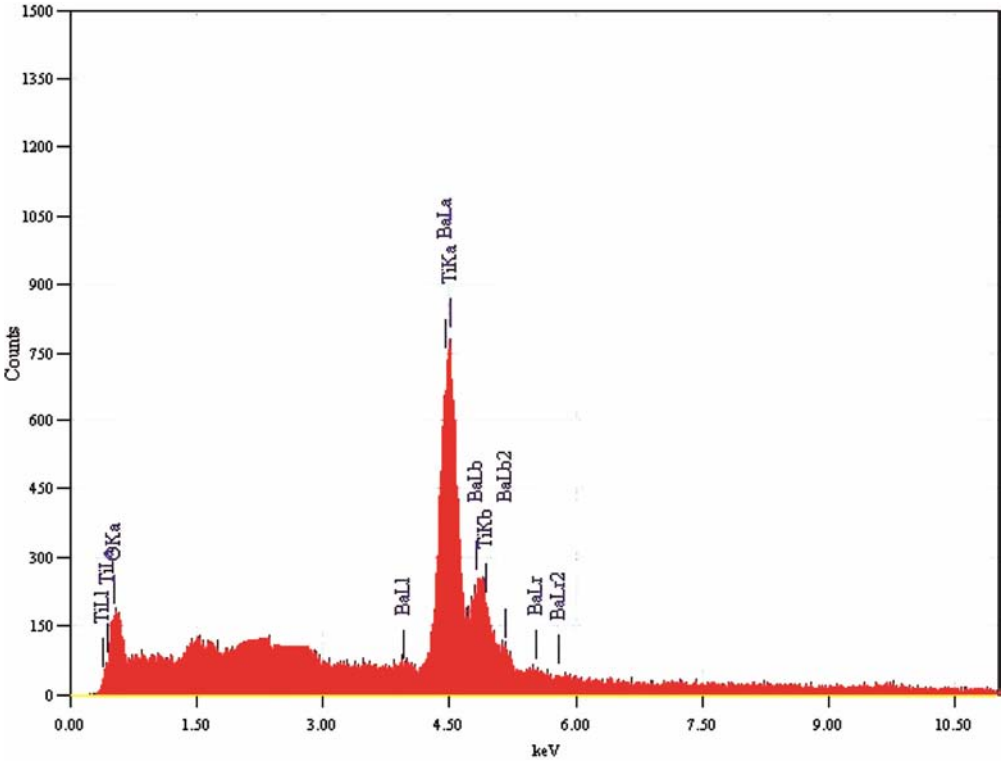

Fig. 3 — EDX spectrum of $BaTiO_3$ powder calcined at 900 °C

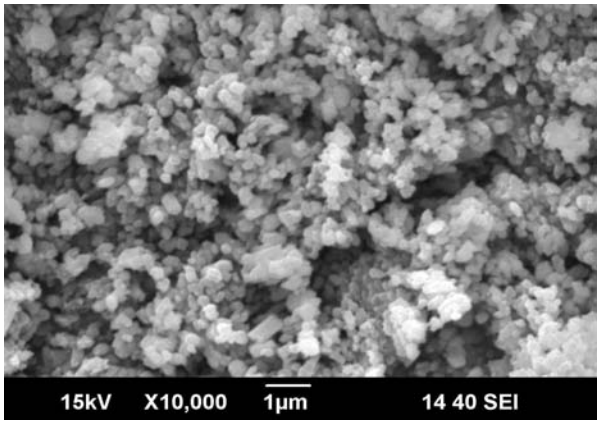

Fig. 4 — SEM image of the $BaTiO_3$ powder calcined at 500 ˚C

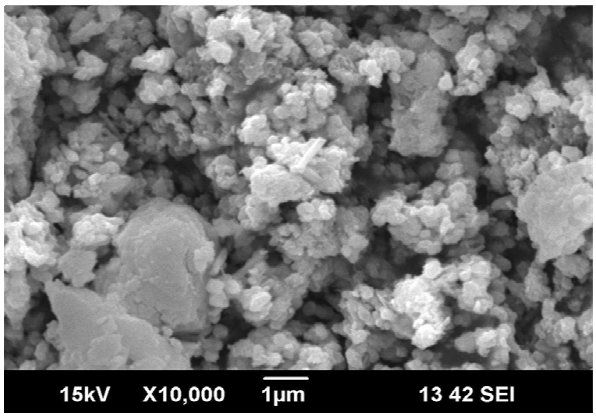

Fig. 5 — SEM image of the $BaTiO_3$ powder calcined at 700 ˚C

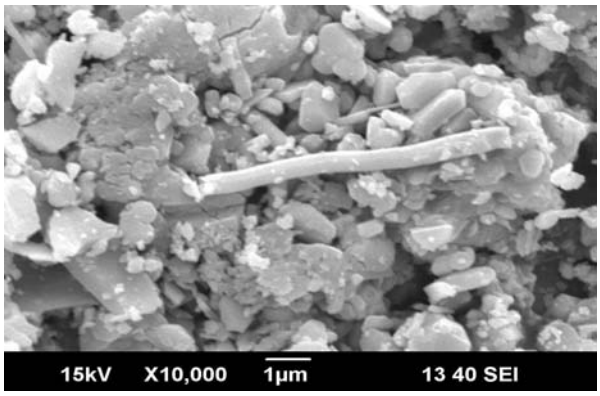

Fig. 6 — SEM image of the $BaTiO_3$ powder calcined at 900 ˚C

shown by separation peaks (200) and (002) at an angle of $2\theta = 44^\circ$ to 46°, which can be seen in Figs 8 and 9.

At 900 ˚C calcined $BaTiO_3$ powder, the peak splitting was found clearly at an angle around $2\theta = 44^\circ$ to 46°, which shows its high degree of

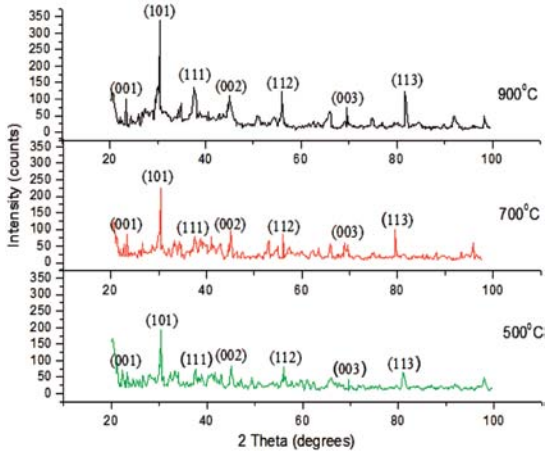

Fig. 7 — XRD spectrum of $BaTiO_3$ powder calcined at different temperatures

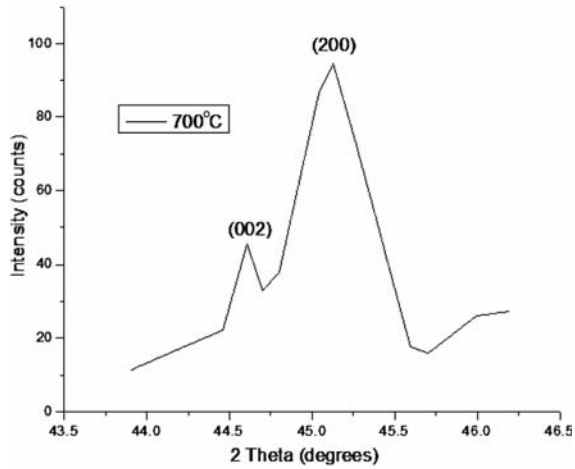

Fig. 8 Tetragonal peak splitting of $BaTiO_3$ powder calcined at 700 ˚C

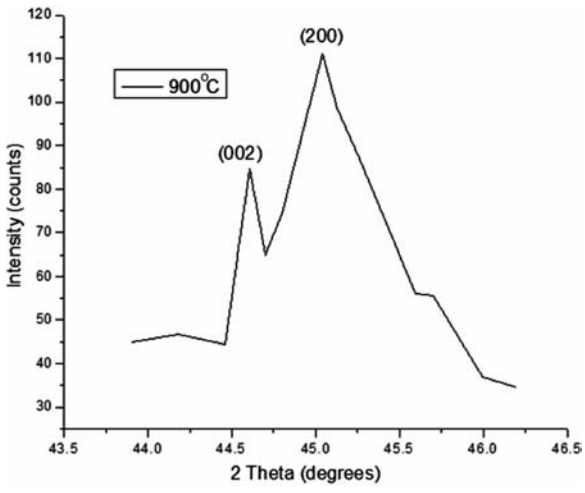

Fig. 9 — Tetragonal peak splitting of $BaTiO_3$ powder calcined at 900 ˚C

Table 1 — Structural parameters calculation of calcined $BaTiO_3$ powder at different temperatures

Calcination Temprature (°C)	2θ (degrees)	hkl	Crystallite size (D) (nm)	Strain (ε) 10^{-3} $lin^{-2}m^4$	Dislocation density (δ) 10^{15} lin/m^2
500	31.50	(101)	44.87	0.917	0.825
700	31.45	(101)	47.61	0.723	0.458
900	31.57	(101)	57.04	0.608	0.308

tetragonality[9, 10, 11]. In the case of 700 °C calcination temperature, there was a small splitting occurring at angle 2θ = 44° to 46°, indicating lesser teragonality[12,13].

The crystallite size is calculated using the Scherrer's formula from the full width half-maximum (FWHM) of the XRD peaks:

$$D = 0.94\lambda/\beta\cos\theta$$

where k is the wavelength of the X-rays used, 2θ is the angle between the incident and scattered X-rays and β is the full width at half maximum. The strain (ε) was calculated from the formula:

$$\varepsilon = \beta\cos\theta/4$$

The dislocation density (δ) is defined as the length of dislocation lines per unit volume of the crystal and is given by:

$$\delta = 1/D^2$$

Table 1 presents the calculated crystallite size (D), dislocation density (δ) and strain (ε) of peaks (101). The crystallite size increases with increase in calcination temperature. $BaTiO_3$ powder calcined at 500 °C has low crystallite size and was found to be around 44.87 nm and it increased to 57 nm at 900 °C calcination temperature. Due to the increase in crystallite size with increasing calcination temperature, the defects in the lattice are decreased, which is turn reduce the internal micro strain and dislocation density.

3.4 Optical properties

Figure 10 shows the reflectance spectra of the $BaTiO_3$ powder for different calcination temperature. It reveals that reflectance decreases with the increase of the calcination temperature, which may be due to increase in crystallite size.

From the reflected spectra the Extinction co-efficient (k) can be calculated from the relation:

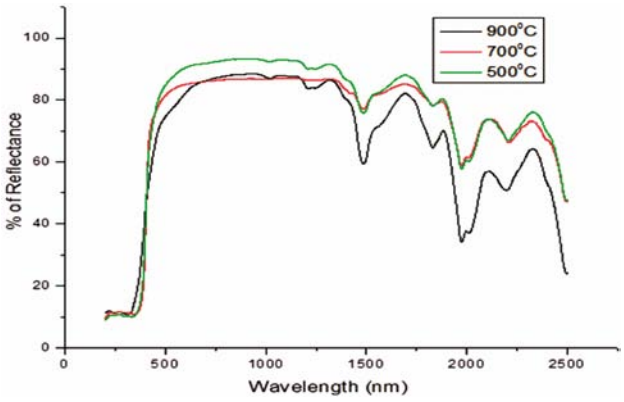

Fig. 10 — Reflectance spectra of the $BaTiO_3$ powder calcined at different temperatures

$$k = 2.303\lambda\log_{10}(1/T)/4\pi d$$

Where d is the thickness of the particles and λ is wavelength of the light and the absorption co-efficient (α) can be calculated by using the expression

$$\alpha = 4\pi k/\lambda$$

Figure 11 shows the variation of Extinction coefficient (k) with wavelength at various calcination temperature. It is seen that Extinction coefficient increases with increase of calcination temperature, which may be due to the improvement in the crystallinity with the minimum imperfections.

Figure 12 shows the variation of absorption coefficient with wavelength at various calcination temperature. The absorption coefficient increases as wavelength decreases[14]. In addition, the absorption coefficient increases with increase in calcination temperature, which is an expected inverse nature of the reflectance spectra.

The absorption coefficient and photon energy are related by the expression:

$$\alpha h\nu = A\,(h\nu - E_g)^n$$

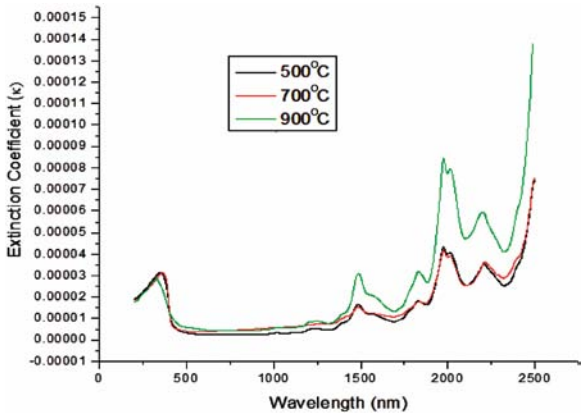

Fig. 11 — Variation of extinction coefficient (k) with wavelength at different calcinations temperature

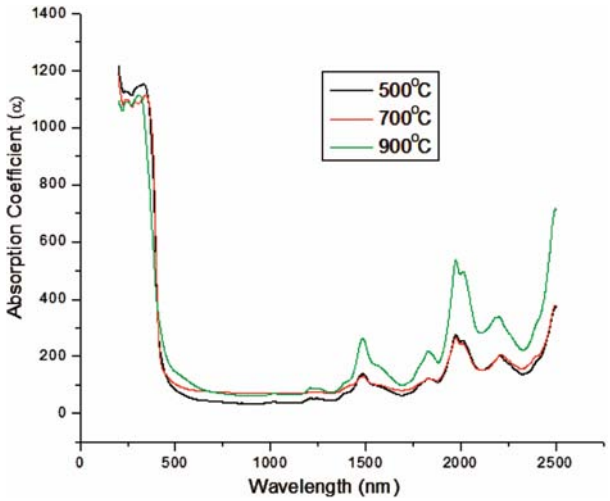

Fig. 12 — Variation of absorption coefficient with wavelength at different calcinations temperature

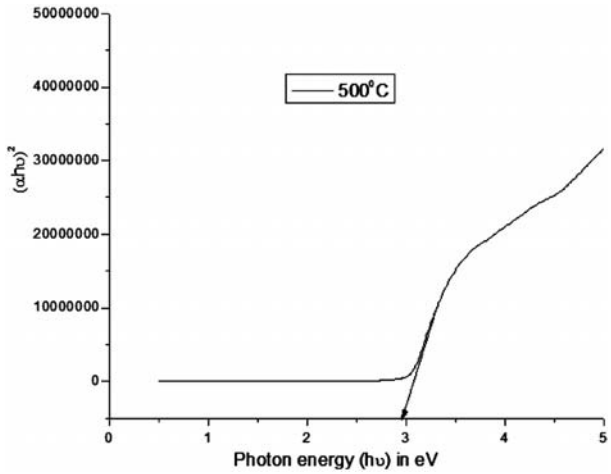

Fig. 13 — Variation of $(\alpha h\nu)^2$ versus photon energy ($h\nu$) of $BaTiO_3$ powder calcined at 500 ˚C

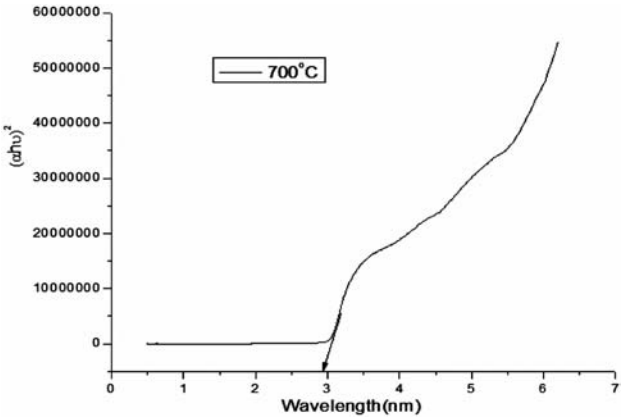

Fig. 14 — Variation of $(\alpha h\nu)^2$ versus photon energy ($h\nu$) of $BaTiO_3$ powder calcined at 700 ˚C

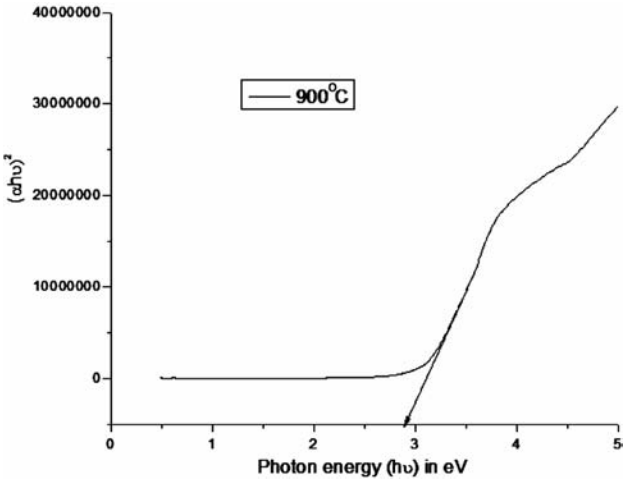

Fig. 15 — Variation of $(\alpha h\nu)^2$ versus photon energy ($h\nu$) of $BaTiO_3$ powder calcined at 900 ˚C

Table 2 — Temperature dependence on optical band gap

Temperature (˚C)	Band gap (eV)
500	2.973
700	2.941
900	2.915

where A is a constant and E_g the optical band gap energy. The variation of $(\alpha h\nu)^2$ versus photon energy ($h\nu$) at 500 ˚C, 700 ˚C and 900 ˚C calcination temperatures is respectively shown in Figs 13-15. From the plot, it is concluded that the optical reflectance in these powder is direct and allowed. It is observed that the band gap decreases with increase in calcination temperature as shown in Table 2. It is found to be in good agreement with the earlier investigations on $BaTiO_3$ powder[15]. The decrease in

the band gap may be due to many reasons. It may be due to the increase of crysrallite size, decrease in strain, decrease in dislocation density and quantum confinement effect.

4 Conclusions

We have successfully synthesized $BaTiO_3$ powders by low cost wet chemical method using commercially available chemicals such as oxalic acid, TiO_2 and $BaCl_2$. The composition of $BaTiO_3$ powders was confirmed by EDS analysis. XRD showed cubic structure for samples calcined at 500 ˚C, whereas samples calcined at 700 ˚C and above showed tetragonal structure. Nanoparticles spherical and rod like in shape were found in SEM. From the reflection spectra, the reflection is found to decrease with increase of calcination temperature. The absorption co-efficient and extinction coefficient of the powders were determined from optical reflection spectra which increase with increase in calcination temperature. The optical band gap of $BaTiO_3$ powders was found to be direct and allowed. A decreasing trend in the optical band gap energy was observed with increase of calcination temperature.

References

1 Burfoot Jack C, *Ferroelectrics*, D Vannostrand Company Ltd, London, (1967).

2 Kao Chen-Feng & Yang Wein-Duo, *Appl Organomet Chem*, 13 (1999) 383.

3 Sreenivasulu A, Prasad TNVKV & Suddhudu, *Indian J Pure and Appl phys*, 45 (2007) 741.

4 Vinothini V, Sigh Paramanard & Balasubramanian M, *Ceramics Inernational*, 32 (2006) 99-103.

5 Mimura Ken-ichi & Yogo Toshinobu, *J of the Ceramic Society of Japan*, 119 (2011) 776.

6 Shaikh A S & Vest G M, *J Am Ceram Soci*, 69 (1986) 682.

7 Boulos M, Fritsch S, Mathieu F, Durand B, Lebey T & Bley V, *Solid State Ionics*, 176 (13) (2005) 1301.

8 Manzoor U & Kim D K, *J Mater Sci Technol*, 23(5) (2007) 655.

9 Begg Bruce D, Vance Eric R, Nowotny & Janusz, *J Am Ceram Soci*, 77(12) (1994) 3186.

10 Stojannovic B D, Simoes A Z & Paiva – Santos C O, *J Eur Ceram Soc*, 25 (2005) 1985.

11 Wada S, Narahata M & Hoshina T, *J Mater Sci*, 38 (2003) 2655.

12 Zee J H, Nersisyan H H, Lee H H & Won C W, *J of Material Science*, 39 (2004) 1397.

13 Yanping Mao, Shaoua Mao, Zuo – Guang Ye, Zhaoxiong Xie & Lansun zhang, *J of Materials Chem & Phys*, 124 (2010) 1232.

14 Jinbao Xu, Jiwei Zhai, Xi Yao, Jianqiang Xue & Zhiming Huang, *J Sol-Gel Sci Techn*, 42 (2007) 209.

15 Guo Haizhong, Liu Lifeng, Chen Zhenghao, Ding Shuo, Lu Hubin, Jin Kui-Juan, Zhou Yueliang & Cheng Bolin, *Europhys Lett*, 73(1) (2006) 110.